Development of Chemo-Selective Gas Sensors Based on Molecularly Imprinted Polymer-Quartz Crystal Microbalance for Detection of Bioactive Compounds in *Curcuma longa*

Fajar Hardoyono*

Department of Environmental Science, Faculty of Science and Technology, Universitas Islam Negeri Profesor Kiai Haji Saifuddin Zuhri, Jl. A. Yani 40 A, Purwokerto 53126, Indonesia

* ***Corresponding author:***

email: hardoyono@uinsaizu.ac.id

Received: August 20, 2024
Accepted: October 29, 2024

DOI: 10.22146/ijc.99285

Abstract: *Turmeric contains bioactive compounds that are efficacious for human health. A breakthrough of simpler and lower-cost identification techniques is needed to utilize it. This paper aims to investigate the development of chemo-selective gas sensors for identifying α-curcumene, ar-turmerone, curlone, and β-sesquiphellandrene. Four chemo-selective sensors were created using quartz crystal microbalance (QCM) sensors coated with molecularly imprinted polymers to identify each of those compounds. The polymers were prepared using polyacrylic acid, hydrochloric acid, and pure target compounds (α-curcumene, ar-turmerone, curlone, and β-sesquiphellandrene). The turmeric odor from 10 different samples was exposed to QCM sensors. The changing frequency of QCM sensors due to the mass loading of target compounds on the surface of QCM sensors was recorded to analyze the performance of QCM sensors. The result of the principal component analysis showed that the QCM sensors performed well and could distinguish the turmeric samples at five combinations of the compounds. The turmeric sample classification using backpropagation neural networks reached high accuracies, with 97.04% in training and 98.73% in testing datasets. These findings indicate that the employment of sensory analysis using QCM sensors has the prospect of being a complementary technique for identifying bioactive compounds.*

Keywords: *bioactive compounds; chemo-selective sensor; molecularly imprinted polymers; quartz crystal microbalance; turmeric*

■ INTRODUCTION

For more than a hundred years, turmeric (*Curcuma longa* L.) has been well-known as a popular phytomedicine worldwide. Numerous studies have documented the use of plant medicine by prehistoric populations worldwide. In India, turmeric was utilized in religious rituals and as one of the classic Ayurvedic treatments [1-2]. Traditional Chinese society knows turmeric as *Ezhu* [3], and it is commonly used as a component of traditional Chinese medicine for patient treatment with atherosclerosis [4]. Traditional Japanese people also utilize turmeric as an efficacious herbal medicine, an anti-inflammatory and anti-amyloid action, and as a treatment for people with dementia disorder [5]. Traditional people in Thailand use turmeric rhizomes as an herbal medicine to treat health disorders such as acne on the human face [6], antitumor activity, and anti-neuroinflammatory [7]. Meanwhile, the Indonesian people in Java Island utilize turmeric as herbal medicine to treat stomach disorders, liver illness, children's fevers, and hypotriglyceridemia [8], and to alleviate fever and headaches in COVID-19 infection [9].

The benefits of bioactive compounds in turmeric have led to the widespread use of this phytomedicine for therapeutic purposes in the contemporary era [10]. Many scientific journals have reported the potential health benefits of turmeric's bioactive components. Several references reported that turmeric rhizome contains α-curcumene as a bioactive compound that proves efficacious for health treatment for humans with

health disorders such as Parkinson's disease [11-13], antiviral, anti-inflammatory, and antioxidant effects for human cells infected by SARS-CoV-2 virus [14], as well as treatment for Alzheimer disorder [15-16]. In addition, curcumin has the potential for human longevity, anti-aging effect [17], neuroprotective effect [18], and inhibits the growth of cancer cells [19-20] and digestive disorders [21].

In addition to curcumin, other research findings show that other bioactive compounds in turmeric, such as ar-turmerone, curlone, and β-sesquiphellandrene are also effective. Ar-turmerone has been investigated as a bioactive compound that exhibits anti-malignant, anti-aging, and anti-inflammatory properties [22]. Furthermore, a bioactive compound in turmeric—i.e., curlone—was found to be productive as a therapeutic agent against ovarian cancer cells [23]. Recent studies have shown that most patients with ovarian cancer have hyper-activated phosphoinositol 3 kinase (PI3K)/protein kinase B (AKT)/mammalian target of rapamycin (mTOR) pathways, which calls for the use of inhibitors. AKT is a serine/threonine kinase previously known as protein kinase B (PKB), which plays a crucial role in primary cellular functions, including cell size and cycle progression. Curlone was investigated for efficacious inhibition of AKT in cancer cells. Meanwhile, β-sesquiphellandrene also has the potential against the SARS-CoV-2 virus. β-sesquiphellandrene inhibits the pathological initiation of the diseases caused by both viruses, namely COVID-19 and severe fever with thrombocytopenia syndrome, by acting not only on the spike protein of SARS-CoV-2 but also on the membrane glycoprotein polyprotein complex of SFTS virus [24].

The experimental methods employed to identify the bioactive compounds in turmeric are crucial in bolstering the scientific data demonstrating the advantages of bioactive compounds in turmeric as the raw material for the pharmaceutical industry. So far, the researcher has employed conventional analytical methods based on Fourier transform infrared (FTIR) spectroscopy [25-26], high-performance liquid chromatography (HPLC) [27-28], and gas chromatography-mass spectroscopy (GC-MS) [29-30] to identify the existence of bioactive compounds in turmeric. Those are precise and potent instruments. However, using those instruments has triggered technical obstacles such as high-cost investment, high electricity consumption, and complex sample pre-treatment. Therefore, a breakthrough in developing a low-cost and more straightforward detection technique is required to simplify the identification of bioactive compounds in herbal medicines.

A chemo-selective template based on a molecularly imprinted polymer-quartz crystal microbalance (MIP-QCM) gas sensor array was developed as a novel approach to target compound identification in *C. longa* L. The QCM is a piezoelectric sensor that, even at small concentrations, is highly sensitive to pressure and mass variation that results from target chemical contact on the crystal surface. This molecular imprinting technique yields target molecules' specific binding sites in the host polymer matrix. The MIP is coated on the surface of the QCM electrode and used as a chemo-selective polymer and susceptible gas sensor. The principle for developing a chemo-selective gas sensor array based on the molecular imprinting technique is designed by creating a cavity inside the polymer layer in which targets of volatile organic compounds are added in a host of polymer matrices. The polymer layer is prepared using specific template molecules capable of identifying target compounds solved in polymer solutions such as polyvinyl chloride [31], polymethacrylic acid [32], ethylene glycol dimethacrylate [33], aminoethanethiol, and 11-mercaptoundecanoic acid [34]. Then, those target compounds are detected from the host polymer matrix by washing, heating, and other chemical procedures.

Previous research has indicated that MIP-QCM sensors can be used to detect a wide range of compounds, including α-terpinene acetate in cardamon [32], andrographolide in the medicinal plant extract [35], and eugenol in clove oil [36]. This research paper, however, investigated the development of a chemo-selective sensor based on MIP-QCM for identifying 4 bioactive compounds in turmeric, namely α-curcumene, ar-turmerone, curlone, and β-sesquiphellandrene in the

turmeric essential oil. This is the first research carried out based on the investigation of earlier studies on related subjects.

Employing a chemo-selective gas sensor based on an MIP-QCM array to identify bioactive compounds in turmeric has the potential to be a breakthrough in exploring the bioactive compounds in turmeric essential oil. A susceptible gas sensor and a selective polymer are used in a more straightforward, less expensive method to identify the target chemicals in turmeric. This investigation synthesized polyacrylic acid (PAA) polymer MIP films with 4 volatile compound templates (α-curcumene, ar-turmerone, curlone, and β-sesquiphellandrene). The target molecules in turmeric essential oil volatile compounds were captured by polymer film deposited on the QCM sensors's surface, which served as chemo-selective layers. The bioactive components of turmeric were identified by measuring the frequency decrease at the QCM sensor array's response. The sensor array responses were analyzed using chemometrics techniques based on principal component analysis (PCA) and back propagation neural networks (BPNN) to identify patterns.

■ EXPERIMENTAL SECTION

Materials

As a source for analytes, the raw material of turmeric rhizomes (*C. longa* L.) was prepared from 10 different traditional markets and purchased around Purwokerto City, Central Java, Indonesia. From each traditional market, we purchased 10 kg of turmeric rhizome. Selection of turmeric rhizome is important to obtain the optimum odor from the turmeric. We purchased the turmeric rhizome, which was still fresh, vaporable, and fragrant. All turmeric rhizomes were cleaned using the water sprayer to get rid of the dirt that stuck to the surface of each rhizome. Following the cleaning process, the rhizomes were then cut to a size of about 1 cm × 1 cm × 0.2 mm and placed in a drying cabinet set at 60 °C for approximately 12 h. The process of slicing and drying the turmeric rhizomes caused its mass to decrease by up to 50%. Hence, only 5 kg of dried turmeric rhizome remained after the slicing and drying process.

Some chemicals used in the experiment included 4 pure compounds (α-curcumene, ar-turmerone, curlone, β-sesquiphellandrene), PAA powder, hydrochloric acid, and ethanol. The α-curcumene and β-sesquiphellandrene were purchased from BenChem, USA, while ar-turmerone and curlone were purchased from RR Chemical, USA. The PAA, hydrochloric acid, and ethanol were purchased from LugChemical, Indonesia. Fig. 1 displays the chemical structures of the pure compounds.

Instrumentation

As shown in Fig. 2, the steam distillation apparatus utilized in this study comprises a gas stove and a stainless boiling chamber with a capacity of 20 L. The boiling chamber has a removable apparatus that holds the slices of turmeric rhizomes above the water level. The apparatus also includes a Graham condenser with a diameter of 2 in and water inlet and outlet nose tubes with a diameter of 3/8 in. The 3/8 in glassware tubes and a faucet adapter are connected to the condenser. A receiver collects the essential oil, and glassware connector

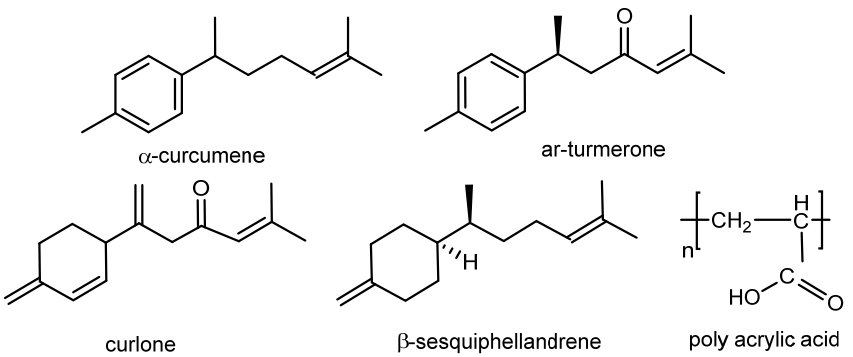

Fig 1. Chemical structure of pure compounds

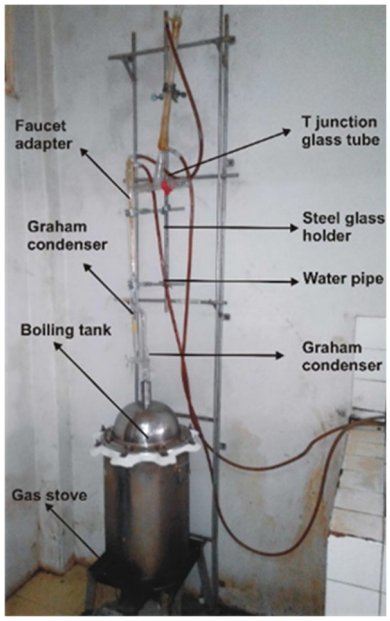

Fig 2. The apparatus of steam distillation for extracting turmeric essential oil

clamps secure the various components. A vertical support rod is included to hold the condenser and receiver upright, and two metal tube clamps are used to secure the condenser.

For a 10 h steam distillation procedure, 5 kg of slices of dried rhizome and 10 L of pure water were put in a 20 L high-pressure boiling tank to obtain pure turmeric essential oil. From each 5 kg of slices of dried turmeric as raw material, approximately 50 mL of essential oil was obtained in the distillation process. Thus, a glass vial holding 100 mL was filled with this essential oil. All steam distillation apparatus, including the boiling tank, Graham condenser, glass connector, and faucet adapter, were cleaned using ethanol. This procedure is repeated to complete 10 turmeric samples in the distillation process. The slicing, drying, and steam distillation processes for 10 turmeric rhizomes were carried out independently to keep odor and volatile compounds from cross-contamination.

Four 9-MHz AT-cut QCM sensors from Seiko Eg&G, Japan, were prepared to create chemo-selective templates. The sensors were embedded between vacuum-deposited Au electrodes. Based on references from previous studies similar to this experiment, 9-MHz AT-cut QCM sensors have been utilized in some experiments to identify target compounds [37-38]. During those studies, 9-MHz AT-cut QCM sensors demonstrated good sensitivity in identifying the target substances in the gas phase. The following is Sauerbrey's equation in Eq. (1) [39], which explains how mass loading causes a decrease in the frequency of the QCM sensor when the target bioactive compounds of turmeric are trapped in the MIP template;

$$\Delta f = \frac{-2f_0^2 \Delta m}{\sqrt{A\left(\mu_g d_g\right)}} \quad (1)$$

where f_0 = initial frequency, μ_g = shear modulus, d_g = density, A = surface area of the coated gold electrode, and Δm = mass loading of QCM.

All QCM sensors were encased in a box-shaped sensing chamber and set inside a cylindrical crystal holder. Four QCM sensors coated in a particular polymer were inserted and configured within the chamber as a sensor array. Three fan systems, a sample container, a flow meter, a controller system, a data collecting system, and a QCM analyzer were among the additional components of the sensor array equipment. The F_1, F_2, and F_3 fan systems operated autonomously by using Arduino controller commands. F_2 was set to pass through the volatile gas of turmeric essential oil into the sensor chamber. In contrast, F_1 and F_3 were set to flow ambient air into a sample container and sensor chamber, respectively. Two flow meters, one within the sample container and the other inside the sensing chamber, were used to manually adjust the flow rates of the ambient air and the smell sample. The data acquisition system recorded the frequency change during the interaction between the fragrance sample and the MIP-QCM sensor. The data was then sent to the QCM analyzer (QCA 922, Seiko EG&G, Japan), fitted with the WinQCM software. Following that process, the computer received the sensor response data to identify patterns.

The Shimadzu GC-MS-QP-2010 (Kyoto, Japan) with auto-sampler Agilent 7683b and MSD Agilent 5975C mass spectroscopy was used to identify the target compounds in the analytes. The QP 2010 SE mass spectrometer (Compaq-Pro Linear data system, class 5 K software) was connected to the GC-MS. The type of column used was Agilent-DB-1 column (30 m × 0.25 mm × 0.2 μm) film thickness Crossband R

100% dimethylpolysiloxane. The column was operated under the following conditions: it was first programmed to operate at 70 °C, and after 10 min, then it was raised to 250 °C (at a rate of 18 °C/min). The injector and detector were operated at 250 and 270 °C, respectively. The injection volume of the sample was designed to be 1 µL for each sample. The mass conditions were as follows: full scan mode in the 30–450 amu mass ranges with 0.2 s/scan, ionization voltage (70 eV), ion source temperature (200 °C), and helium carrier velocity (30 cm/s). Compounds were identified using the NIST 08 database (NIST mass spectrum database, PC version 2008), WILEY 8, and FFNSC1.3 (Flavor & Fragrance & Synthetic Compounds) libraries. Based on the percentages of the region displayed in the GC-MS spectra, a computerized integrator determined the number of main chemicals. The GC-MS analysis used similar procedures for identifying the concentration of 4 target compounds for 10 turmeric essential oil samples.

Procedure

Volatile constituents' identification using GC-MS

To identify the major constituents in 10 samples of turmeric essential oil, 5 µL of turmeric essential oil was injected into the GC-MS column using a micro-syringe (Nichipet Ex, Japan). The chromatography process using GC-MS was assigned for 60 min. The relative percentage amount of each compound was determined by comparing the ratios of the peak area and the total areas. This procedure was repeated for 10 samples (TEO_1-TEO_{10}).

Creation of a chemo-selective polymer layer

A set of chemo-selective polymer layers consists of 4 QCM sensors coated with different MIP films. The procedure for coating a set of MIP film was carried out utilizing the methodology [40-41] as follows. Four polymer solutions were prepared by dissolving 500 mg of PAA in 20 mL of ethanol. The solution was divided into 4 different glass vials, namely vial glass A, B, C, and D. Each mixture of PAA and ethanol solution was added with 20 µL of α-curcumene, ar-turmerone, curlone, and β-sesquiphellandrene for vial glass A, B, C, and D using micro syringe, respectively. Each solution was added with 50 µL of hydrochloric acid. The polymer solutions were stirred for 6 h using a magnetic stirrer (As one, Japan). After that, 10 µL of polymer solution from vial glass A, B, C, and D was dropped on the surface of the QCM electrode (one side only). Every QCM electrode coated with MIP polymer droplets was put in a spin coating (500 rpm for 1 min) separately to obtain a few hundred nm of MIP coating. The MIP template molecule was placed in the oven at a temperature of 40 °C for 24 h to dislodge the pure compounds from the polymers and create the cavities of pure compounds in chemo-selective templates.

The quartz crystal only received one side of the MIPs polymer droplet. The quartz crystal's other side was used to create the contact with electrodes to send the electric signal. The rubber case was used to seal the other side of the quartz crystal, preventing it from coming into touch with the MIP solution to minimize the error in the sensing process. The QCM sensor coated with MIP can be used for a single experiment due to the mass loading of the target compound on the QCM surface. Afterwards, the surface of the QCM sensor must be cleaned using ethanol in the ultrasonic cleaner to reuse the target compound detection. The employment of an MIP-coated QCM sensor that has been used for previous target compound detection is not recommended because it may cause a decreased sensitivity in the target compound detection process. Hence, for the detection of target compounds in 10 samples of with 10 times replication in measurement, a 10×10 set of QCM sensors coated with different MIPs must be prepared. The design for creating 10 sets of 4 QCM sensors coated with a polymer layer using the same technique is presented in Fig. 3.

Sensing mechanism process

The schematic diagram presents component devices to develop chemo-selectives based on the MIP-QCM sensor array shown in Fig. 4. Turmeric essential oils were placed in a 100 mL Pyrex glass bottle with a microfluidic closure. Two Teflon tubes are attached to the microfluidic closure. The first tube is used to flow pure and dry air for dilution, while the other is utilized to pass through turmeric odor into QCM templates. Previously, inert nitrogen was used to clean the microfluidic closure

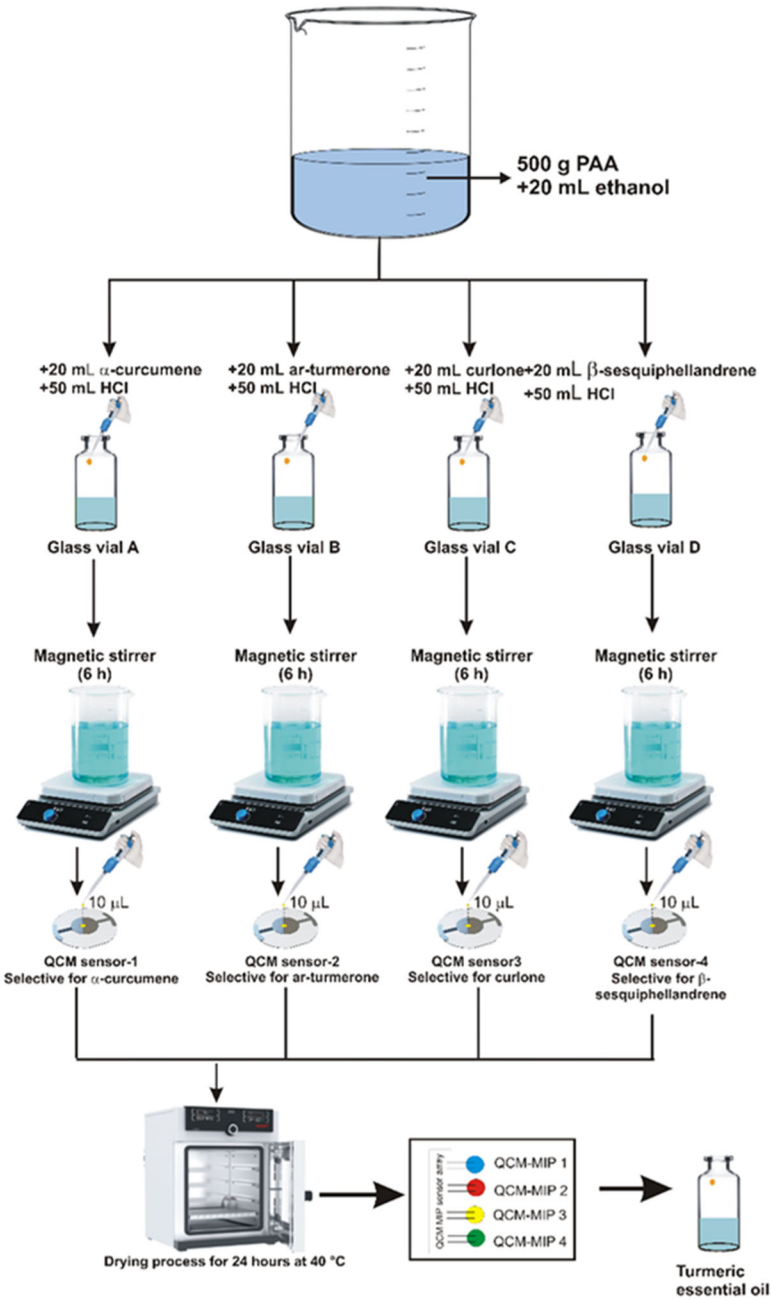

Fig 3. The process for MIP preparation for creating chemo-selective sensors towards α-curcumene, ar-turmerone, curlone, and β-sesquiphellandrene as the target compounds

and plastic tube to prevent odor contamination from other turmeric samples or the room environment. A 2 × 2 cm piece of cotton paper was placed inside a Pyrex glass vial. Then, 25 µL of turmeric essential oil was dropped on the surface of cotton paper. The Arduino controller system managed the autonomous operation of the air pump F_1, F_2, and F_3 to support the sensing process. For 60 s, F_1 was turned on while F_2 and F_3 were turned off. After that, 1 L of pure dry air was flown into a Pyrex glass bottle to dilute the turmeric essential oil odor concentration within the Pyrex glass bottle. Afterwards, the F_2 was turned on while the F_1 and F_3 were turned off. The volatile gas of turmeric essential oil was then subjected to sensory analysis. Therefore, three cycles of

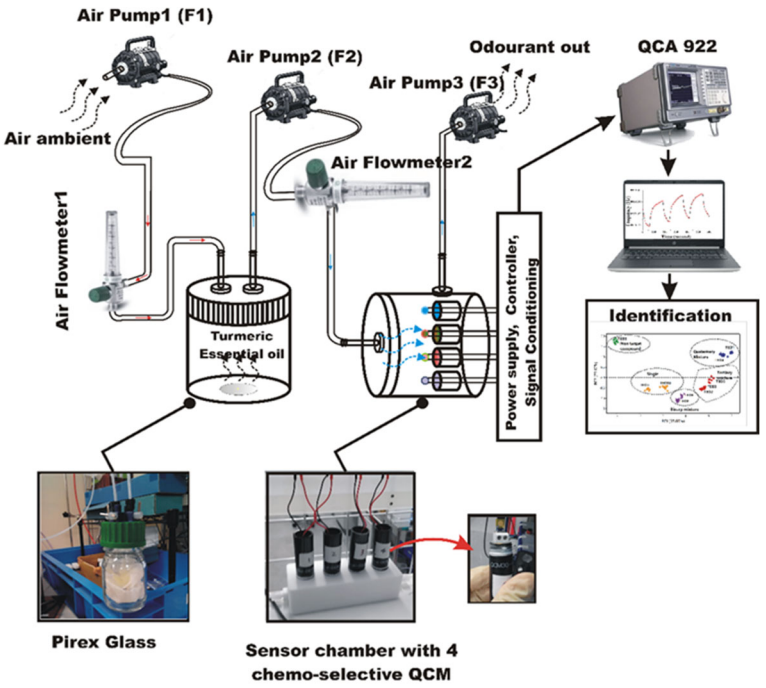

Fig 4. The schematic diagram of an electronic device for identifying bioactive compounds in turmeric using chemo-selective sensor based on MIP-QCM gas sensor array

sensory analysis were allocated to measure the MIP-QCM response.

The cycle measurement time was set at 60 s, of which 30 s were allocated to flow the turmeric odor into the sensor chamber (the detecting phase), and another 30 s were assigned to the cleaning phase (passing a clean air sensor into the sensor chamber to waste the volatile gas of turmeric in chemo-selective sensor). In every sensing phase, F_2 was turned "ON", and F_3 was turned "OFF" by the control unit. The target smell was transferred from a Pyrex glass bottle to the sensor chamber, which included 4 QCM electrodes coated with MIPs at a flow rate of 1 L/min using the F_2 pump. To get the best concentration in the sensor chamber, we set the flow rate to 1 L/min. Our investigations showed that when the clean air flow rate in the F_1 pump was set to more than 1.5 L/min, saturation volatile chemicals were produced in the sensor chamber. The sensor chamber's minimal concentration of volatile chemicals was observed when the flow rate was set to less than 0.5 L/min.

When the target odor was flown into the sensor chamber, the mass loading of the target compound inside the chemo-selective polymer layer over the QCM sensor caused the frequency of the QCM electrode to decrease. In the cleaning phase, the control unit F_2 was set to "OFF", and F_3 "ON" was set to "ON". The target odor was disclosed from the sensor chamber through outlet holes. The mass loaded surrounding the chemo-selective polymer layer decreased. As a result, the QCM sensor's frequency increased. These sensory procedures are repeated to measure the frequency decrease and increase for each cycle measurement due to mass loading over the chemo-selective polymer layers to measure 10 turmeric samples with 10 times replication.

■ RESULTS AND DISCUSSION

Identification of Target Bioactive Compounds Using GC-MS

The GC-MS analysis of 10 samples of turmeric essential oil identified several major compounds with different concentrations. The list of them is shown in Table 1. Four target compounds—i.e., α-curcumene, ar-turmerone, curlone, and β-sesquiphelladrene—were detected in concentrations over 15% in $TEO_{1\text{-}10}$ except TEO_9. In samples TEO_1 and TEO_4, the concentrations of 4 compounds identified were more than 15%. In samples

Table 1. List of major constituents in 10 turmeric essential oil samples using GC-MS

Compound name	Abundance (%)									
	TEO_1	TEO_2	TEO_3	TEO_4	TEO_5	TEO_6	TEO_7	TEO_8	TEO_9	TEO_{10}
α-curcumene	23.45	35.60	25.40	24.10	30.50	36.00	1.65	49.20	4.50	3.90
Ar-turmerone	28.40	29.40	33.60	29.80	33.40	45.20	62.40	30.50	3.20	65.40
Borneol	2.84	-	1.64	2.45	0.45	1.89	1.54	1.34	29.75	2.10
Curlone	15.50	23.50	28.45	15.60	28.40	2.45	-	-	3.80	-
Ethyl *p*-methoxicinnamate	1.10	2.13	1.65	5.65	1.56	1.60	-	1.20	40.20	-
β-sesquiphellandrene	27.40	-	2.64	18.60	3.40	2.50	1.23	2.10	1.45	2.10

TEO_2, TEO_3, and TEO_5, the concentrations of α-curcumene, ar-turmerone, and curlone were more than 15%. The compounds of α-curcumene and ar-turmerone identified were more than 30% in $TE0_6$ and $TE0_8$. In samples TEO_7 and TEO_{10}, ar-turmerone is the single compound identified in more than 62%. Meanwhile, the target compounds—i.e., α-curcumene, ar-turmerone, curlone, and β-sesquiphelladrene—were identified as less than 5% in sample TEO_9 due to its primary components—i.e., predominantly borneol and ethyl-*p*-methoxycinnamate, which were analyzed as non-target chemicals in this experiment.

The turmeric's distinct odor is generated by ketonic sesquiterpenes: α-curcumene, ar-turmerone, curlone, and β-sesquiphellandrene. GC-MS chromatograms reveal variations in the quantity of these analytes. The amount of α-curcumene was the highest in sample TEO_8 (49.20%) and the lowest in sample TEO_7 (1.65%), whereas ar-turmerone concentration ranged from 3.20% in samples TEO_9 to 62.40% in sample TEO_7. The compound of curlone was identified only in seven samples (TEO_1–TEO_6 and TEO_9). Meanwhile, the compound of β-sesquiphellandrene was identified in more than 15% concentration in samples TEO_1 and TEO_4.

Fig. 5(a-d) visualizes the typical frequency change of the chemo-selective MIP-based QCM sensor array for Sensor 1, Sensor 2, Sensor 3, and Sensor 4 in three measurement cycles, respectively. A cycle measurement consisted of sensing and cleaning phases. The down curve indicates the sensing phase when the volatile compounds of turmeric essential oil were passed through into chemo-selective templates. The hydrogen bonding between the –CHO groups of hydrocarbons in the target compounds and the –COOH group of PAA polymer coated on the surface of the QCM sensor caused the mass loading in the chemo-selective templates. Hence, the frequency of the QCM sensor decreased as formulated by Sauerbrey's equation in Eq. (1).

Furthermore, the upcurve in Fig. 5 visualizes the cleaning phase in which the saturated volatile compounds of turmeric essential oil were dislodged from the chemo-selective sensor array. Consequently,

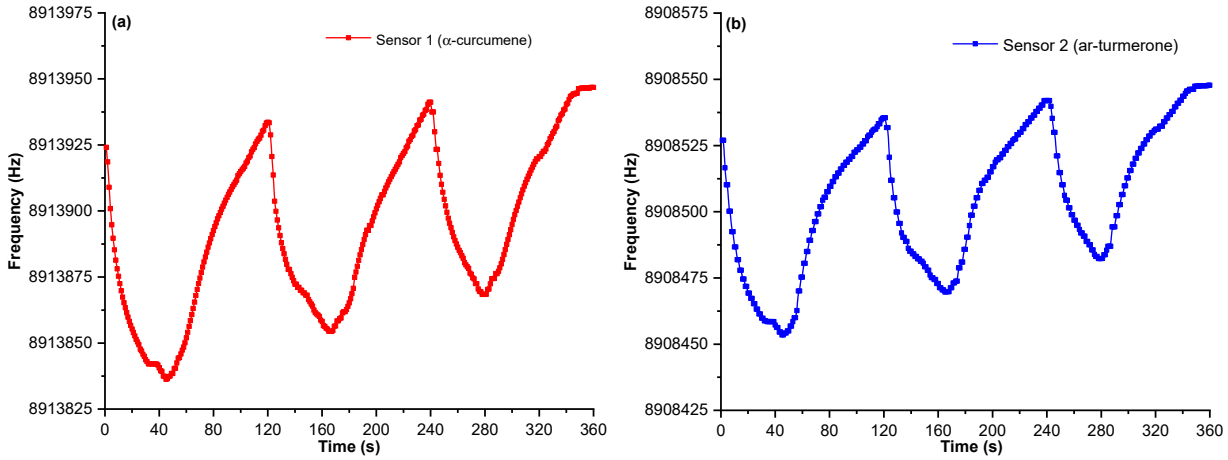

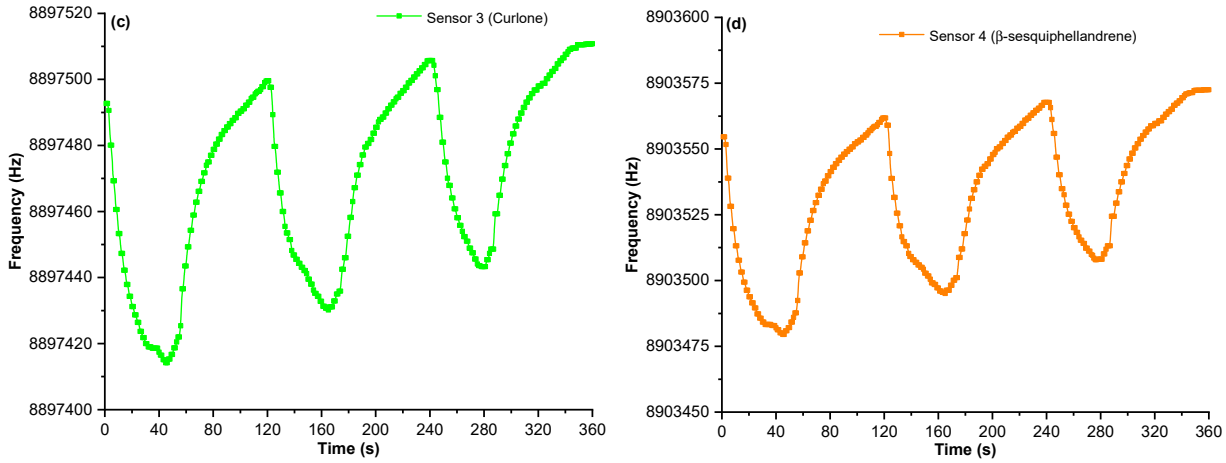

Fig 5. The Typical response of the MIP-QCM sensor array towards turmeric odor exposure at the sample of TEO_1: (a) sensor 1 (α-curcumene), (b) sensor 2 (ar-turmerone), (c) sensor 3 (curlone), (d) sensor 4 (β-sesquiphellandrene)

the hydrogen bonding between the –CHO groups in the target compounds with the –COOH group of PAA polymer on the chemo-selective sensors coated on the surface of the QCM sensor was disclosed. The frequency of the MIP-based QCM sensor increased. The duration of the sensing and cleaning phases was assigned to 30 s.

Fig. 6 visualizes the principle of bioactive identification of α-curcumene using the chemo-selective templates based on the MIP-QCM sensor array. The procedure for heating the QCM sensor coated with the polymer of PAA in the oven at a temperature of 40 °C for 12 h caused the dislodgment of α-curcumene. Then, the dislodgment caused the cavities of α-curcumene trace in the chemo-selective layer on the surface of the QCM sensor. When the turmeric odor passed through in the sensing phase, the adsorption of α-curcumene occurred in the MIP cavities and caused mass loading on the surface of the QCM sensor. Then, the frequency of the QCM sensor decreases.

Meanwhile, when the turmeric odor was removed from the sensor array, the mass loading of α-curcumene on the surface of the chemo-selective layer was diminished.

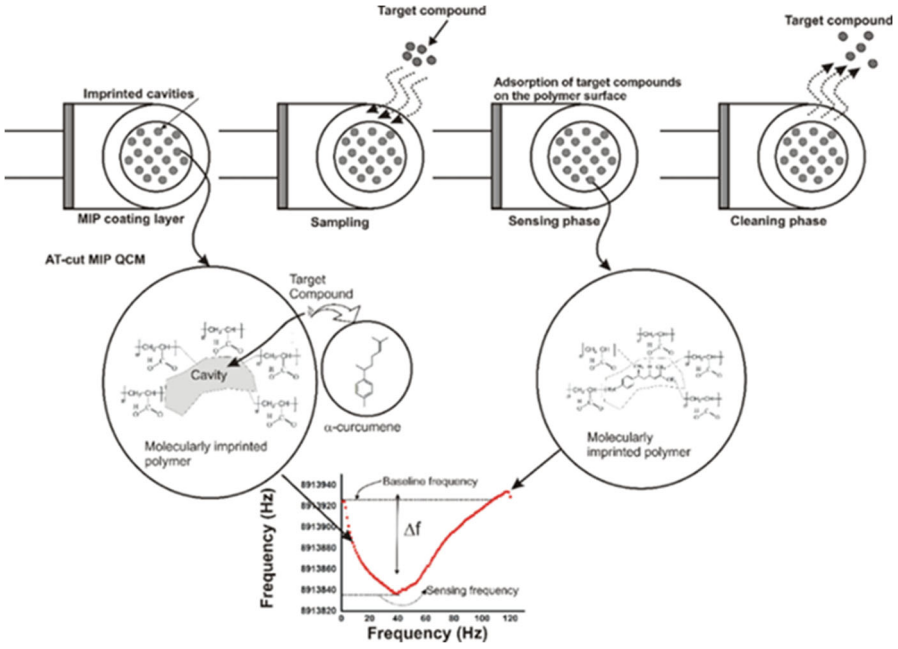

Fig 6. The Schematic of the MIP recognition principle of a-turmerone using an MIP-based QCM sensor

Hence, the QCM sensor's frequency returned to its baseline level. The measurement of frequency decrease due to the mass loading for all turmeric essential oil samples was replicated 10 times to analyze the sensor selectivity and repeatability towards the target compounds.

As shown in Fig. 5, the frequency changes of QCM sensors due to the mass loading of target compounds in Sensors 1–4 were presented in 3 measurement cycles. A cycle measurement consisted of sensing and cleansing phases, respectively. However, detecting target compounds by observing the frequency change of mass loading of target compounds on the surface of QCM sensors in the 2nd and 3rd cycles has the possibility of decreasing sensor sensitivity. While running the cleaning phase in the 2nd cycle, the mass loading of the target bioactive compound trapped in the QCM surfaces was not disclosed ideally. Hence, the mass loading of target compounds in the QCM surface did not attach ideally while running the sensing phase in the 2nd cycle measurement.

Based on this condition, the measurement of frequency changes as the main parameter for target bioactive compound detection in Sensors 1–4, respectively, involved only measurement in the 1st cycle. The frequency changes in Sensors 1–4, respectively, recorded in the 2nd and 3rd measurements, were not used for data analysis. As shown in Table 2, the sensitivity displays the value of frequency decrease (Δf) obtained from measuring 10 samples of turmeric odor with 10 times replication.

The Δf obtained from the MIP-QCM sensor array response measured in the first cycle is displayed in Table 2. The adsorption of target compounds with the chemo-selective layer on the QCM sensor's surface generated 5 frequency change variation patterns. First, the frequency change among 4 sensors indicated more than 9 Hz when the samples of TEO_1 and TEO_2 were measured. In sample TEO_1, Δf value in Sensor 1 (α-curcumene) was estimated at 9.23 ± 0.06 Hz. Meanwhile, the Δf values of Sensors 2 (ar-turmerone), Sensor 3 (curlone), and Sensor 4 (β-sesquiphellandrene) were measured at 9.46 ± 0.07, 8.80 ± 0.14, and 8.82 ± 0.30 Hz, respectively. The same pattern of Δf values in sample TEO_1 occurred in sample TEO_4. The result of Δf measurement for Sensors 1–4 showed 8.78 ± 0.15, 9.00 ± 0.15, 7.87 ± 0.16, and 8.01 ± 0.14 Hz, respectively. Based on the Δf values, it was indicated that turmeric essential oil from samples TEO_1 and TEO_4 contained the mixture of quaternary mixture.

Second, TEO_2, TEO_3, and TEO_5 samples show similar frequency change patterns in Sensors 1–3. The Δf values in these sensors were recorded as more than 8.00 Hz. However, the Δf values in Sensor 4 were indicated as low. The Δf values for Sensor 4 in samples TEO_2, TEO_3, and TEO_5 were recorded as less than 2.06 Hz. It showed that turmeric essential oil in samples TEO_2, TEO_3, and TEO_5 contained the tertiary mixture of α-curcumene, ar-turmerone, and curlone. Third, samples of turmeric essential of TEO_6 and TEO_8 have similar patterns in frequency change in Sensors 1 and 2. In these samples, the Δf values in Sensors 1 and 2 were high and recorded more than 9.10 Hz. Meanwhile, Sensors 3 and 4 were measured at less than 1.00 Hz. It is indicated that the turmeric essential oil in samples TEO_6 and TEO_8 contained the binary mixture of α-curcumene and ar-turmerone. Fourth, when the turmeric essential oil from samples TEO_7 and TEO_{10} were passed through in the surface of chemo-selective templates, the Δf values in only Sensor 2 were recorded as more than 9.80 Hz. Other sensors were measured at less than 3.3 Hz. Based on the Δf values, the turmeric essential oil from samples TEO_7 and TEO_{10} contained ar-turmerone as the target bioactive compound. Fifth, When the turmeric essential oil from sample TEO_9 was flown in chemo-selective templates, the Δf values from all sensors were low, ranging from 0.46 ± 0.18 to 0.52 ± 0.26 Hz. The low values of Δf in all sensors showed that all target compounds were non-detected by Sensors 1–4.

The adsorption of target compounds with the chemo-selective layers on the surface of QCM sensors can be predicted by comparing the Δf values of 4 QCM sensors. Adsorption of target chemicals with chemo-selective layers happened if the Δf was high. As shown in Table 2, the MIP-QCM sensor array measured 0.17 ± 0.08 Hz for the minimum and 9.88 ± 0.13 Hz for

Table 2. Data frequency changes (Δf) obtained from nine types of turmeric odor with 10 times repetition

Sample code	Δf + s (Hz)			
	Sensor 1	Sensor 2	Sensor 3	Sensor 4
TEO_1	9.23 ± 0.06	9.46 ± 0.07	8.80 ± 0.14	8.82 ± 0.30
TEO_2	9.48 ± 0.06	9.10 ± 0.10	8.00 ± 0.11	0.17 ± 0.08
TEO_3	9.11 ± 0.11	9.39 ± 0.05	8.78 ± 0.20	0.44 ± 0.27
TEO_4	8.78 ± 0.15	9.00 ± 0.15	7.87 ± 0.16	8.01 ± 0.14
TEO_5	9.19 ± 0.19	9.25 ± 0.12	9.30 ± 0.14	2.06 ± 0.48
TEO_6	9.11 ± 0.13	9.40 ± 0.14	1.29 ± 0.51	0.80 ± 0.30
TEO_7	0.39 ± 0.17	9.83 ± 0.15	0.40 ± 0.18	0.47 ± 0.20
TEO_8	9.68 ± 0.08	9.41 ± 0.09	0.22 ± 0.11	0.37 ± 0.12
TEO_9	0.46 ± 0.18	0.47 ± 0.25	0.62 ± 0.20	0.52 ± 0.26
TEO_{10}	3.06 ± 0.59	9.88 ± 0.13	1.75 ± 0.11	1.43 ± 0.24

the maximum frequency change with the standard of deviation values (Δf ± s). The experiment results showed that the minimum frequency change Δf at which all sensors could detect the target compounds was 5.0 Hz. If the recorded value of Δf was more than 5.00, Sauerbrey's equation indicated that the cavity absorbed a particular target molecule in the MIP-QCM template. It caused a frequency shift and a loading mass in the coating of the sensor layer. Nevertheless, if the recorded value of Δf was less than 5.00, no adsorption of a specific target molecule with a polymer matrix occurred.

The threshold at Δf values, which indicates the adsorption of target compounds, is more than 5.00 Hz (Table 2). In contrast, the adsorption of target substances with a chemo-selective layer did not happen when the Δf was low, less than 5.00 Hz. Based on the data of Δf values in all sensors in turmeric essential oil from samples of TEO_1–TEO_{10}, a quaternary mixture was absorbed by Sensors 1–4. A tertiary mixture of α-curcumene, ar-turmerone, and curlone was absorbed by Sensors 1–3. A binary mixture of α-curcumene and ar-turmerone was absorbed by Sensors 1 and 2, while only a single compound of ar-turmerone was absorbed by Sensor 2. These findings affirmed the GC-MS data tabulation shown in Table 1, which showed that samples of TEO_1 and TEO_4 contain α-curcumene, ar-turmerone, curlone, and β-sesquiphellandrene. TEO_2, TEO_3, and TEO_5 samples contain α-curcumene, ar-turmerone, and curlone. Samples of TEO_6 and TEO_8 contain α-curcumene and ar-turmerone, while the samples of TEO_7 and TEO_{10} contain only α-curcumene, ar-turmerone, curlone, and β-sesquiphellandrene. Meanwhile, sample TEO_9 did not contain α-curcumene, ar-turmerone, curlone, and β-sesquiphellandrene. Furthermore, non-target compounds, including borneol and ethyl *p*-methoxycinnamate, appeared in GC-MS.

Principal Component Analysis (PCA)

Multivariate analysis based on PCA was used to measure the performance of the chemo-selective sensor array. The performance of the chemo-selective gas sensor array to identify 4 target compounds in 10 samples of turmeric essential is represented by the score plot of principal component analysis shown in Fig. 5. PCA is a multivariate statistical technique used to detect patterns in data and describe the data in a different format to highlight variations and similarities among patterns [42]. PCA reduces the number of correlated variables in a data set by using a smaller number of uncorrelated variables to represent the principal component. PCA was used to eliminate the number of data dimensions without significantly changing the original data. Employment of PCA is carried out due to the difficulty of detecting a pattern in a high dimension of data. By employing PCA, a set of sensor array responses is transformed into two components.

The PCA algorithm converts a set of correlated variables with each other into a new set of uncorrelated variables [43]. The initial coordinate corresponds to the primary component (PC_1) derived from the largest

eigenvalue. The second coordinate represents the second principal component (PC_2) derived from the second-highest eigenvalue. There is no correlation between PC_1, PC_2, and PC_n. The ordering of PC_1, PC_2, and PC_n is based on the variance they capture in the data set, with PC_1 having the most relative to PC_2. PC_2 has the highest amount of volatility in the dataset compared to PC_3. Employment of PCA reduces the variables obtained from concurrent measurements by lowering the number of data dimensions. However, diminishing the data's dimensions does not lose information since PCA's primary objective is to acquire PC_1 and PC_2, which possess the highest eigenvalues, to preserve the data's properties. The method for identifying the target bioactive compound of turmeric essential oil involved 10 samples with 10 times replication and yielded a robust data dimension. Hence, PCA is needed to measure the performance of chemo-selective sensors and determine the composition of bioactive compounds in the analytes based on the frequency change value released by all sensors.

The PCA score plot that visualizes the separation of 10 turmeric essential oil samples measured using a chemo-selective gas sensor array in two principal component coordinates (PC_1 and PC_2) is presented in Fig. 7. As shown in Fig. 7, a total of 100 output responses obtained from measurement of 10 turmeric essential oil samples with 10 times replication are separated into 5 different groups. The PC_1 and PC_2 obtained a 55.60% and 23.10% variance, respectively. The first group includes 20 responses from samples of TEO_1 and TEO_4 containing the quaternary mixture. The second group consists of 30 responses obtained from samples TEO_2, TEO_3, and TEO_5 containing the tertiary mixture of α-curcumene, ar-turmerone, and curlone, respectively. Twenty responses from samples TEO_6 and TEO_8 containing the binary mixture of α-curcumene and ar-turmerone are placed in the third group. The fourth group consisted of 20 responses from samples TEO_7 and TEO_{10}, containing only ar-turmerone. Meanwhile, 20 responses from TEO_9 containing nontarget compounds are separated into the fifth group.

The sensitivity of the chemo-selective gas sensor array to distinguish 10 turmeric essential oil samples based on the concentration of target compounds can be visualized using the loading plot. The loading plot displays the correlation coefficients between PC_1 and PC_2. These coefficients are generated by eigenvectors of PC_1 and PC_2. The coefficient values vary between −1 and 1. Coefficients that are close to −1 or 1 indicate a considerable influence of the variable on the component. When the coefficients are near 0, it suggests that the variable has a minimal impact on the component. Calculating the Euclidian distance using the correlation

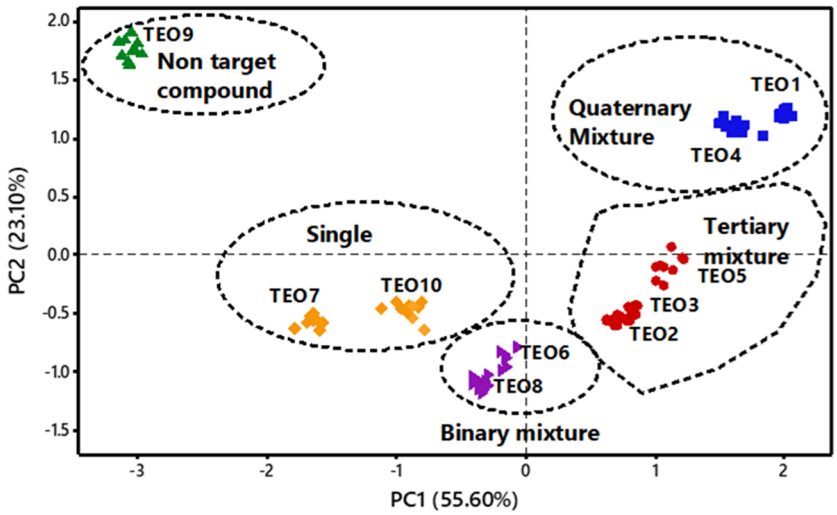

Fig 7. The PCA score plot of PCA that visualizes the separation of 10 turmeric essential oil samples measured using chemo-selective gas sensor array

coefficient value of the first and second principal components can be used to see which variables significantly influence the observables.

From Fig. 8, it can be calculated that the lengths of the loading plot for Sensors 1 and 2 are 0.6204 and 0.7809, respectively. For Sensors 3 and 4, the length of the loading plot is calculated at 0.6225 and 0.7778, respectively. The length of the loading plot among all sensors is almost similar, indicating that all sensors have identical contributions to distinguish the 10 turmeric essential oils based on the concentration of on-target compounds. However, the loading plots for Sensors 2 and 4 are longer than for Sensors 1 and 3, indicating that Sensors 2 and 4 have better sensitivity in identifying ar-turmerone and β-sesquiphellandrene than the other sensors.

Back-Propagation Neural Networks Algorithm

Another method for analyzing the performance of a chemo-selective sensor array to classify the turmeric essential oil based on the composition of target compounds is artificial neural networks based on a BPNN. BPNN uses a supervised learning approach based on the delta or Widrow-Hoff rule to identify the target. Machine learning architecture based on the BPNN algorithm needs an input layer, one or more hidden layers, and an output layer. In addition, the performance of BPNN for classifying turmeric samples according to the target compounds' composition depends on multiple factors, including data features, network architecture, network initialization, the transfer function in the hidden and output layers, the training algorithm, the learning rate or learning epoch (η), and error-goal (ε).

The Matlab R2010a (MathWorks, Inc., USA) software was used to train and test datasets of chemo-selective output response. The architecture design of the BPNN networks used to classify the turmeric essential oil samples is displayed in Fig. 9. The BPNN method employed three-layer conventional neural networks: (1) four neuron nodes in the input layer; (2) 12 neuron nodes in the hidden layer; and (3) two neuron nodes in the output layer. The input layer for the BPNN was inputted by the Δf values acquired from the four MIP-QCM sensors. Binary code was used to identify the different classes of the sample as follows. Group 1 was designated as turmeric samples containing a quaternary mixture; Group 2 was designated as turmeric samples containing tertiary mixture α-curcumene, ar-turmerone, and curlone; Group 3 was designated as turmeric samples containing binary mixture α-curcumene and ar-turmerone; Group 4 was designated as turmeric samples containing single target compound of ar-turmerone; and Group 5 was designated as turmeric samples without any target compound. The binary sigmoid activation function activates the hidden and output layer neurons.

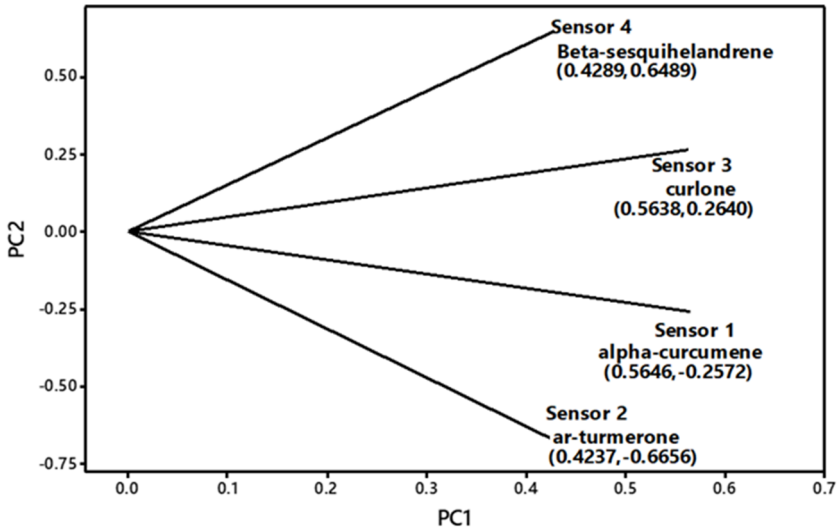

Fig 8. The loading plot of PCA that visualizes the performance of four chemo-selective gas sensors to identify the specific target compound

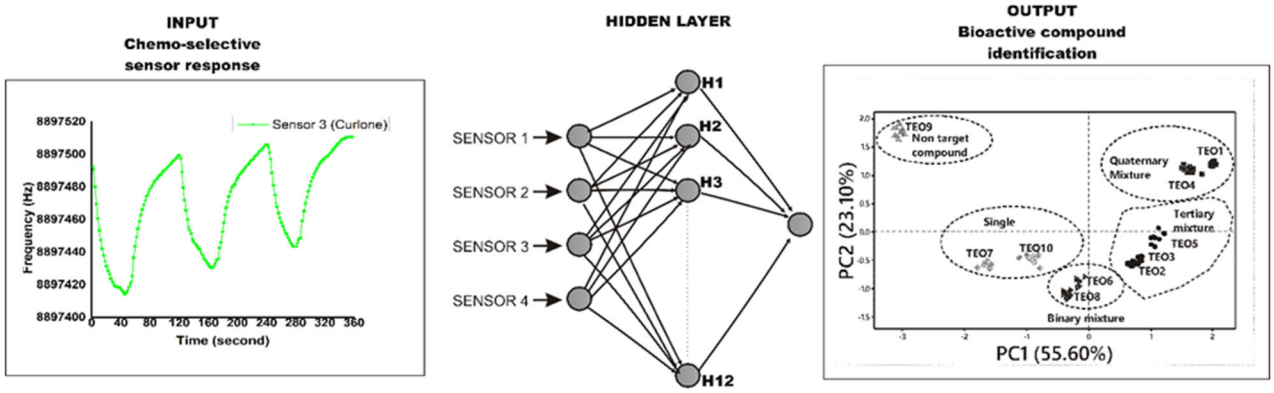

Fig 9. The architecture design of BPNN used to classify the turmeric essential oil samples based on the composition of target compounds

The output responses obtained from the measurement of 10 samples of turmeric essential oil with 10 replications were prepared for running BPNN. A hundred output responses were divided into two groups: (1) the training data set comprising 70 responses and (2) the testing data set consisting of 30 responses. Initial random weights of values between −1 and 1 were assigned throughout the learning phase. The BPNN training process used several parameter values to get the minimum, i.e., maximum epoch = 1,000, learning rate ($\eta = 0.1$), and means square error ($< 10^{-4}$). After 2,514 iterations, the training of BPNN reached a mean square error of 10^{-4}. The confusion matrix used to classify 100 chemo-selective output responses divided into 70 testing data sets and 30 training data sets, respectively, is displayed in Table 3. Since a sample from TEO_{10} that should have been classified was mistakenly classified as a binary mixture sample class and a sample from TEO_8 and TEO_{10} that should have been classified was mistakenly classified as a single target compound sample class, the accuracy of the projected samples from the testing data set reached 97.14%. In comparison, the sample classification accuracy from the training data set reached 96.66%.

Additionally, k-fold cross-validation was used as another technique to measure the BPNN machine classifier's performance. The performance of the BPNN classifier for sample classification utilizing 70 training data samples and 30 testing data samples with 10-fold cross-validation is displayed in Table 3. The k^{th}-fold validation, which ranges from k-fold of 1 to 10, was averaged to determine the classifier's performance. Table 3 shows that the BPNN classifier's average accuracy for the training and testing datasets was 97.04% and 98.73%,

Table 3. BPNN classifier performance using 10-fold-cross validation for sample classification

k^{th} fold	Training data set (70 samples)		Testing data set (30 samples)	
	Correct class	Incorrect class	Correct class	Incorrect class
1	68 samples	2 samples	30 samples	-
2	68 samples	2 samples	28 samples	2 samples
3	69 samples	1 sample	28 samples	2 samples
4	70 samples	-	29 samples	1 sample
5	68 samples	2 samples	30 samples	-
6	70 samples	-	30 samples	-
7	69 samples	1 sample	28 samples	2 samples
8	69 samples	1 sample	28 samples	2 samples
9	68 samples	2 samples	29 samples	1 sample
10	70 samples	-	29 samples	1 sample

respectively. The BPNN classifier achieved 100% accuracy in training data sets for k-fold of 4, 6, and 10, and testing data sets for k-fold of 1, 5, and 6, respectively. A sample was misclassified in the training for k-fold of 4, 6, and 10, as well as for testing data sets k-fold of 4, 9, and 10, respectively. The remaining two samples were categorized in the wrong classes in the training data set using k-fold of 2, 2, 5, and 9, as well as the testing data set using k-fold of 2, 3, 7, and 8, respectively.

A matrix with all diagonal elements at 100% and all off-diagonal elements at 0% is classified using an ideal classifier. Table 3 shows that most samples were accurately identified while using BPNN as a machine classifier. The ratio of correctly identified samples to all test samples (the average of diagonal elements in the classification matrix) is used to calculate the average classification rate, which is 97.04% accurate for the testing dataset and 98.73% for the training dataset. The binary, tertiary, quaternary, and non-target classes are the four classes into which the BPNN networks accurately classified the response from the MIP-QCM sensor array, as shown in Table 3.

Selectivity, Accuracy, and Feasibility of MIP-QCM Sensors

QCM sensors coated with different MIPs have shown good sensitivity and selectivity for the detection of target compounds. Data analysis results using PCA and BPNN compared to GC-MS analysis showed good selectivity and accuracy of QCM sensors for the detection of those target compounds. The selectivity of QCM sensors for detecting target analytes can be explored using the value of frequency changes that occur in the QCM sensor while interacting with the turmeric essential oil samples as the analytes. The screening of major constituents of all turmeric essential oil samples indicates that all turmeric essential oil samples contained different compositions of volatile compounds. However, 4 target compounds were identified in various concentrations. In other words, a turmeric essential oil sample had different concentrations of 4 target compounds. It can contain quaternary, tertiary, binary, or a single composition of those compounds.

The QCM sensor array coated with different MIPs was employed to identify whether the turmeric essential oil samples contained quaternary, tertiary, binary, or single composition. The design of the chemo-selective sensor array was only selective toward single target compounds. To assure the single selectivity, 4 QCM sensors were coated with a thin layer created using polymer and 4 pure compounds. After the polymerization process, the pure compounds were removed from the layer and got the MIP templates, which are selective to a single target compound. Furthermore, the MIP templates were used to capture the single target compound. Capturing non-target compounds is almost impossible because non-target compounds have molecules with different structures than pure compounds. Hence, the cavity of the pure compound in each MIP template is only suitable for the single target compound.

The MIP-QCM sensor selectivity can be observed using the frequency changes values in the QCM sensor analyzer. Based on the data experiment, the frequency changes recorded in all MIP-QCM sensor measurements varied from 0.2 to 9.9 Hz. Based on Saurbreuy's equation in Eq. (1), the frequency changes of the MIP-QCM sensor is proportional to the mass loading of target compounds. This means that the higher the concentration of target compounds, the higher the potential to create mass loading on the surface of MIP templates. Based on data analysis using 10 turmeric essential oil samples with 10 replications, the frequency change of QCM sensors was recorded from 1.0 to 9.8 Hz, depending on the concentration of target compounds.

Meanwhile, the frequency change was recorded as less than 1.0 Hz when the mass loading of target compounds did not occur in the MIP template. Visualization in the coordinate of principal components (PC1 versus PC2) describes the selectivity of MIP-QCM sensor array towards 10 samples of turmeric essential oil with different compositions of target compounds. In the coordinate of principal components, 10 samples of turmeric essential oil were divided into 4 groups based on the similarity of target compounds identified using MIP-QCM gas sensors.

MIP-QCM gas sensors also showed high accuracy for target compound identification. The performance of

MIP-QCM sensors measured by BPNN algorithms and validated by GC-MS analysis shows the accuracy of MIP-QCM sensors. Using 100 measurements, MIP-QCM reached more than 96% accuracy in identifying the target compounds. This means that from a 100-time sensing analysis, 96 times the MIP-QCM gas sensor array identified the target compounds with the right prediction compared to the GC-MS analysis result. Only 4 times, the MIP-QCM gas sensor array identified the target compounds with the wrong prediction compared to the GC-MS analysis result.

Based on the analysis data, a chemo-selective gas sensor array based on MIP-QCM is prospective to be developed as a more straightforward, low-cost, low-energy consumption for detecting bioactive compounds in turmeric samples. The simplicity of the instruments can be seen from the apparatus used in experiments. The apparatus comprises 4 QCM coated with MIPs, a headspace system, a frequency analyzer, and supported devices (power supply, signal conditioning, controller, and data acquisition). The process for creating the coating of QCM is also simple. The PAA, HCl, and pure compound polymer solution were used to drop each QCM sensor. Afterward, it was dried in a vacuum to remove the pure analytes. The process of bioactive compound identification is also straightforward. The essential oil samples were put in a bottle equipped with a cap. The headspace system works autonomously to flow the volatile gas into the QCM sensor chamber to measure the frequency decrease due to the interaction between bioactive compounds and the QCM sensor coated with MIPs for selective target analytes.

In addition, the investment and electric cost for running detection of bioactive compounds using a chemo-selective gas sensor array based on MIP-QCM is cheaper compared to other detection methods using GC-MS, HPLC, FTIR, and UV-vis spectrophotometer. Employment of standard methods using those instruments requires more expensive purchasing and maintaining the instruments. The electric consumption for running the MIP-QCM gas sensor array is below 500 W h^{-1}. The electric power consumption for running the MIP-QCM sensor array apparatus is lower than that for running GC-MS, HPLC, FTIR, and UV-vis spectrophotometer. Even using more straightforward and lower-cost instruments, the detection of bioactive compounds using a MIP-QCM sensor array reaches high accuracy. The target compounds detection experiment using 100 samples of turmeric essential oil obtained more than 96% accuracy. Based on the data experiment, the detection method of bioactive compounds using MIP-QCM is prospective to be developed as an alternative method for bioactive compounds since it is not only simpler and highly accurate but also lower cost.

■ CONCLUSION

Four chemo-selective sensor templates have been developed to identify 4 target bioactive components in 10 samples of turmeric essential oil, namely α-curcumene, ar-turmerone, curlone, and β-sesquiphellandrene. GC-MS analysis confirmed these chemicals' presence in nine turmeric samples. Sensory analysis of 10 turmeric essential oil samples showed good chemo-selective gas sensor array performance for identifying the target compounds. Analysis of output sensor response using PCA and BPNN showed high performance of chemo-selective sensor array for identifying the target compounds in the analytes. The quaternary mixture was identified in samples TEO_1 and TEO_4. A tertiary mixture of α-curcumene, ar-turmerone, and curlone was identified in TEO_2, TEO_3, and TEO_5 samples. A binary mixture of α-curcumene and ar-turmerone was identified in TEO_6 and TEO_9 samples, while a single target compound of ar-turmerone was identified in samples TEO_7 and TEO_{10}, respectively. Meanwhile, no target compound was detected in sample TEO_9. The analysis using the BPNN algorithm for classifying 10 turmeric essential oil samples based on the composition of target bioactive compound reached 97.04% accuracy for the testing dataset and 98.73% for the training. In comparison, another classifying BPNN technique using 10-fold-validation reached 97.04% and 98.73% accuracy in training and testing datasets, respectively. The most responsive and selective sensors are Sensors 2 and 4, which measure ar-turmerone and β-sesquiphellandrene.

Low concentrations of target or non-target compounds imprinted in polymer layers are difficult for the QCM sensor to detect. Based on data analysis, which showed high performance in the experiment, the employment of a chemo-selective sensor array can be utilized as a quick and precise method to identify the different bioactive chemicals in other herbal medicines.

■ ACKNOWLEDGMENTS

The researchers thank the Institute of Research and Community Services UIN Professor Kiai Haji Saifuddin Zuhri, Purwokerto, for granting the research fund under Contract No. 812/2022.

■ CONFLICT OF INTEREST

There is no conflict of interest to declare.

■ REFERENCES

[1] Wardani, R.S., Schellack, N., Govender, T., Dhulap, A.N., Utami, P., Malve, V., and Wong, Y.C., 2023, Treatment of the common cold with herbs used in Ayurveda and jamu: Monograph review and the science of ginger, liquorice, turmeric and peppermint, *Drugs Context*, 12, 2023-2-12.

[2] Peram, M.R., Jalalpure, S.S., Joshi, S.A., Palkar, M.B., and Diwan, P.V., 2017, Single robust RP-HPLC analytical method for quantification of curcuminoids in commercial turmeric products, Ayurvedic medicines, and nanovesicular systems, *J. Liq. Chromatogr. Relat. Technol.*, 40 (10), 487–498.

[3] Lin, L., Zhou, X., Gao, T., Zhu, Z., Qing, Y., Liao, W., and Lin, W., 2024, Herb pairs containing *Curcumae Rhizoma* (Ezhu): A review of bio-active constituents, compatibility effects and t-copula function analysis, *J. Ethnopharmacol.*, 319 (3), 117199.

[4] Ma, B., Yang, S., Li, J., Wen, Z., Ouyang, H., Zhang, W., Feng, Y., and He, M., 2021, Therapeutic targets and biological mechanisms of curcumol on atherosclerosis: A study based on network pharmacology approach and biological studies, *Pharmacogn. Mag.*, 17 (74), 216–222.

[5] Komiyama, M., Ozaki, Y., Wada, H., Yamakage, H., Satoh-Asahara, N., Kishimoto, A., Katsuura, Y., Imaizumi, A., Hashimoto, T., Sunagawa, Y., Morimoto, T., and Hasegawa, K., 2022, Study protocol to determine the effects of highly absorbable oral curcumin on the indicators of cognitive functioning: A double-blind randomised controlled trial, *BMJ Open*, 12 (9), e057936.

[6] Khumsupan, P., and Gritsanapan, W., 2013, "Selected Thai Medicinal Plant for the Treatment of Acne: *Garcinia mangostana* Linn" in *Acne: Etiology, Treatment Options and Social Effects*, Eds. Elsaie, M.L., Nova Science Publishers, Hauppauge, New York, US, 41–68.

[7] Kotwal, G.J., 2009, "Curcumin: A Versatile Nutraceutical and an Inhibitor of Complement" in *Handbook of Nutraceuticals Vol. I: Ingredients, Formulations, and Applications*, Eds. Pathak, Y.V., CRC Press, Louisville, KY, US, 217–221.

[8] Rahmat, E., Lee, J., and Kang, Y., 2021, Javanese turmeric (*Curcuma xanthorrhiza* Roxb.): Ethnobotany, phytochemistry, biotechnology, and pharmacological activities, *Evidence-Based Complementary Altern. Med.*, 2021 (1), 9960813.

[9] Maulida, P.S., and Rahmawati, R., 2022, Self-medication practices for COVID-19 prevention: A study among medical students in Yogyakarta, Indonesia, *J. Res. Pharm.*, 26 (7), 1960–1968.

[10] Jha, C.B., Singh, C., Randhawa, J.K., Kaul, A., Varshney, R., Singh, S., Kaushik, A., Manna, K., and Mathur, R., 2024, Synthesis and evaluation of curcumin reduced and capped gold nanoparticles as a green diagnostic probe with therapeutic potential, *Colloids Surf., B*, 241, 114050.

[11] Bássoli, R.M.F., Audi, D., Ramalho, B.J., Audi, M., Quesada, K.R., and Barbalho, S.M., 2023, The effects of curcumin on neurodegenerative diseases: A systematic review, *J. Herb. Med.*, 42, 100771.

[12] Darbinyan, L.V., Simonyan, K.V., Hambardzumyan, L.E., Simonyan, M.A., Simonyan, R.M., and Manukyan, L.P., 2023, Membrane-stabilizing and protective effects of curcumin in a rotenone-induced rat model of Parkinson disease, *Metab. Brain Dis.*, 38 (7), 2457–2464.

[13] Lei, T., Li, C., Liu, Y., Cui, Z., Deng, S., Cao, J., Yang, H., and Chen, P., 2024, Microfluidics-enabled

mesenchymal stem cell derived neuron like cell membrane coated nanoparticles inhibit inflammation and apoptosis for Parkinson's disease, *J. Nanobiotechnol.*, 22 (1), 370.

[14] Nicoliche, T., Bartolomeo, C.S., Lemes, R.M.R., Pereira, G.C., Nunes, T.A., Oliveira, R.B., Nicastro, A.L.M., Soares, É.N., da Cunha Lima, B.F., Rodrigues, B.M., Maricato, J.T., Okuda, L.H., de Sairre, M.I., Prado, C.M., Ureshino, R.P., and Stilhano, R.S., 2024, Antiviral, anti-inflammatory and antioxidant effects of curcumin and curcuminoids in SH-SY5Y cells infected by SARS-CoV-2, *Sci. Rep.*, 14 (1), 10696.

[15] Pei, J., Palanisamy, C.P., Natarajan, P.M., Umapathy, V.R., Roy, J.R., Srinivasan, G.P., Panagal, M., and Jayaraman, S., 2024, Curcumin-loaded polymeric nanomaterials as a novel therapeutic strategy for Alzheimer's disease: A comprehensive review, *Ageing Res. Rev.*, 99, 102393.

[16] Azzini, E., Peña-Corona, S.I., Hernández-Parra, H., Chandran, D., Saleena, L.A.K., Sawikr, Y., Peluso, I., Dhumal, S., Kumar, M., Leyva-Gómez, G., Martorell, M., Sharifi-Rad, J., and Calina, D., 2024, Neuroprotective and anti-inflammatory effects of curcumin in Alzheimer's disease: Targeting neuroinflammation strategies, *Phytother. Res.*, 38 (6), 3169–3189.

[17] Izadi, M., Sadri, N., Abdi, A., Zadeh, M.M.R., Jalaei, D., Ghazimoradi, M.M., Shouri, S., and Tahmasebi, S., 2024, Longevity and anti-aging effects of curcumin supplementation, *GeroScience*, 46 (3), 2933–2950.

[18] Khayatan, D., Razavi, S.M., Arab, Z.N., Hosseini, Y., Niknejad, A., Momtaz, S., Abdolghaffari, A.H., Sathyapalan, T., Jamialahmadi, T., Kesharwani, P., and Sahebkar, A., 2024, Superoxide dismutase: A key target for the neuroprotective effects of curcumin, *Mol. Cell. Biochem.*, 479 (3), 693–705.

[19] Li, J., Wang, X., Xue, L., and He, Q., 2024, Exploring the therapeutic mechanism of curcumin in prostate cancer using network pharmacology and molecular docking, *Heliyon*, 10 (12), e33103.

[20] Mohd Shafiee, M.A., Syed Alwi, S.S., Hanapi, N.A.I., Salaebing, M., Othman, Z., and Nurdin, A., 2024, Cytotoxicity, proliferation and migration effects of 2,6-bis-(4-hydroxyl-3-methoxybenzylidine)cyclohexanone (BHMC) on human liver cancer, HepG2 cells, *Malays. J. Med. Health Sci.*, 20 (3), 174–185.

[21] Thavorn, K., Wolfe, D., Faust, L., Shorr, R., Akkawi, M., Isaranuwatchai, W., Klinger, C., Chai-Adisaksopa, C., Tanvejsilp, P., Nochaiwong, S., Straus, S.E., and Hutton, B.A., 2024, Systematic review of the efficacy and safety of turmeric in the treatment of digestive disorders, *Phytother. Res.*, 38 (6), 2687–2706.

[22] Flores, G., 2017, *Curcuma longa* L. extract improves the cortical neural connectivity during the aging process, *Neural Regener. Res.*, 12 (6), 875–880.

[23] Adedotun, I.O., Abdul-Hammed, M., Egunjobi, B.T., Ismail, U.T., Yusuf, J.Y., Afolabi, T.I., and Gbadebo, I.O., 2024, Identification of novel inhibitors of P13K/AKT pathways: An integrated *in-silico* study towards the development of a new therapeutic agent against ovarian cancer, *Phys. Sci. Rev.*, 9 (7), 2469–2498.

[24] Joshi, A., Sunil Krishnan, G., and Kaushik, V., 2020, Molecular docking and simulation investigation: Effect of beta-sesquiphellandrene with ionic integration on SARS-CoV2 and SFTS viruses, *J. Genet. Eng. Biotechnol.*, 18 (1), 78.

[25] Indu, B., and Thanigaivel, S., 2023, Identification of bioactive compounds from black pepper and turmeric extracts and their antioxidant, antibacterial activity structural confirmation by GC-MS and FT-IR for feed formulation, *AIP Conf. Proc.*, 2587 (1), 130044.

[26] Sahne, F., Mohammadi, M., Najafpour, G.D., and Moghadamnia, A.A., 2017, Enzyme-assisted ionic liquid extraction of bioactive compound from turmeric (*Curcuma longa* L.): Isolation, purification and analysis of curcumin, *Ind. Crops Prod.*, 95, 686–694.

[27] Choi, Y., Kim, W., Lee, J.S., Youn, S.J., Lee, H., and Baik, M.Y., 2020, Enhanced antioxidant capacity of puffed turmeric (*Curcuma longa* L.) by high

hydrostatic pressure extraction (HHPE) of bioactive compounds, *Foods*, 9 (11), 1690.

[28] Hornung, P.S., Masisi, K., Malunga, L.N., Beta, T., and Ribani, R.H., 2018, Natural bioactive starch film from Amazon turmeric (*Curcuma longa* L.), *Polym. Bull.*, 75 (10), 4735–4752.

[29] Oyinlola, K.A., Ogunleye, G.E., Balogun, A.I., and Joseph, O., 2024, Comparative study: Garlic, ginger and turmeric as natural antimicrobials and bioactives, *S. Afr. J. Sci.*, 120 (1-2), 1–7.

[30] Kirmani, F., Saddiqe, Z., Saleem, S., Ali, F., and Haq, F.U., 2024, Phytochemical investigation and antibacterial activity of *Curcuma longa* against multi-drug-resistant bacteria, *S. Afr. J. Bot.*, 164, 137–145.

[31] Lowdon, J.W., Eersels, K., Rogosic, R., Boonen, T., Heidt, B., Diliën, H., van Grinsven, B., and Cleij, T.J., 2019, Surface grafted molecularly imprinted polymeric receptor layers for thermal detection of the new psychoactive substance 2-methoxphenidine, *Sens. Actuators, A*, 295, 586–595.

[32] Debabhuti, N., Neogi, S., Mukherjee, S., Dhar, A., Sharma, P., Vekariya, R.L., Sarkar, M.P., Tudu, B., Bhattacharyya, N., Bandyopadhyay, R., and Muddassir, M., 2021, Development of QCM sensor to detect α-terpinyl acetate in cardamom, *Sens. Actuators, A*, 319, 112521.

[33] Prabakaran, K., Jandas, P.J., Luo, J., Fu, C., and Wei, Q., 2021, Molecularly imprinted poly(methacrylic acid) based QCM biosensor for selective determination of L-tryptophan, *Colloids Surf., A*, 611, 125859.

[34] Tsuru, N., Kikuchi, M., Kawaguchi, H., and Shiratori, S., 2006, A quartz crystal microbalance sensor coated with MIP for "bisphenol A" and its properties, *Thin Solid Films*, 499 (1), 380–385.

[35] Shafiqul Islam, A.K.M., Krishnan, H., Ahmad, M.N., Nadaraja, P., and Helal Uddin, A.B.M., 2021, Novel molecular imprint polymer quartz crystal microbalance nanosensor for the detection of andrographolide in the medicinal plant extract, *Russ. J. Electrochem.*, 57 (6), 671–679.

[36] Banerjee, M.B., Chowdhury, S.R., Roy, R.B., Tudu, B., Ghosh, M., Pramanik, P., and Bandyopadhyay, R., 2021, Development of a low-cost portable gas sensing system based on molecularly imprinted quartz crystal microbalance sensor for detection of eugenol in clove oil, *IEEE Trans. Instrum. Meas.*, 70, 2001110.

[37] Devkota, J., Kim, K.J., Ohodnicki, P.R., Culp, J.T., Greve, D.W., and Lekse, J.W., 2018, Zeolitic imidazolate framework-coated acoustic sensors for room temperature detection of carbon dioxide and methane, *Nanoscale*, 10 (17), 8075–8087.

[38] Ichinohe, S., Tanaka, H., and Kanno, Y., 2007, Gas sensing by AT-cut quartz crystal oscillator coated with mixed-lipid film, *Sens. Actuators, B*, 123 (1), 306–312.

[39] Ding, X., Li, J., Chen, X., Zhang, J., and Zhu, M., 2022, Derivation for mass-frequency relationship of a quartz crystal microbalance based on an equivalent circuit network analysis method, *IEEE Trans. Instrum. Meas.*, 71, 9510208.

[40] Jha, S.K., and Hayashi, K., 2015, A quick responding quartz crystal microbalance sensor array based on molecular imprinted polyacrylic acids coating for selective identification of aldehydes in body odor, *Talanta*, 134, 105–119.

[41] Jha, S.K., Liu, C., and Hayashi, K., 2014, Molecular imprinted polyacrylic acids based QCM sensor array for recognition of organic acids in body odor, *Sens. Actuators, B*, 204, 74–87.

[42] Benesty, J., Huang, G., Chen, J., and Pan, N., 2024, "Principal Component Analysis in Noise Reduction and Beamforming" in *Microphone Arrays*, Springer, Cham, Switzerland, 57–85.

[43] Gupta, A., Wazir, S., Mahto, A.K., and Alam, S.I., 2023, "Facial Recognition Using Principal Component Analysis" in *Artificial Intelligence & Blockchain in Cyber Physical Systems: Technologies & Applications*, Eds. Arif, M., Balas, V.E., Nafis, T., Qureshi, N.M.F., Wasir, S., and Hussain, I., CRC Press, New Delhi, India, 1–10.